
ODOV: Towards Open-Domain Open-Vocabulary Object Detection

Yupeng Zhang

College of Intelligence and Computing
Tianjin University
Tianjin, China 300350
zhangyupeng@tju.edu.cn

Ruize Han

Faculty of Computer Science and Control Engineering
Shenzhen University of Advanced Technology
Shenzhen, China 518107
rz.han@siaat.ac.cn

Fangnan Zhou

College of Intelligence and Computing
Tianjin University
Tianjin, China 300350

Song Wang

Faculty of Computer Science and Control Engineering
Shenzhen University of Advanced Technology
Shenzhen, China 518107

Wei Feng

College of Intelligence and Computing
Tianjin University
Tianjin, China 300350

Liang Wan

College of Intelligence and Computing
Tianjin University
Tianjin, China 300350

Abstract

In this work, we handle a new problem of Open-Domain Open-Vocabulary (ODOV) object detection, which considers the detection model’s adaptability to the real world including both domain and category shifts. For this problem, we first construct a new benchmark OD-LVIS, which includes 46,949 images, covers 18 complex real-world domains and 1,203 categories, and provides a comprehensive dataset for evaluating real-world object detection. Besides, we develop a novel baseline method for ODOV detection. The proposed method first leverages large language models to generate the domain-agnostic text prompts for category embedding. It further learns the domain embedding from the given image, which, during testing, can be integrated into the category embedding to form the customized domain-specific category embedding for each test image. We provide sufficient benchmark evaluations for the proposed ODOV detection task and report the results, which verify the rationale of ODOV detection, the usefulness of our benchmark, and the superiority of the proposed method.

1 Introduction

Object detection is a fundamental task in computer vision, which aims at locating and identifying objects within images. Recent years have witnessed the rapid development of object detection, which, however, is still with unsolved problems for real-world applications. On one hand, due to the labor-intensive and costly manual annotation process for bounding boxes, the annotated object categories in the object detection dataset (for training) are limited, which are certainly smaller than the category vocabulary in the real world (**category shift**). On the other hand, most existing works have primarily focused on handling clear natural images. However, in many real-world scenarios, such as applications for autonomous driving, video surveillance, and Internet search, the captured images are not always of high quality and clarity. Instead, they may be plagued by various types of degradation or style differences (**domain shift**). For instance, the images captured in rainy or foggy weather (from the scene), with low resolution or various noises (during the imaging), or with different artistic styles (Internet data), *etc.*

We find that current research on object detection (OD) in open scenes has noticed the above two problems. Such as the one-shot OD [1, 2, 3, 4], open-world OD [5, 6, 7], and the most recent open-vocabulary OD [8, 9] are designed for the open-category detection problem. Besides, for the open-domain setting, domain adaption, domain generalization have been used for OD task [10, 11, 12, 13, 14, 15, 16], and some image restoration methods are also applied to the downstream OD task [17, 18, 19]. However, these two problems are studied separately. Actually, the *compound category and domain shifts are more common* in real-world scenes. For example, from indoor (training) to outdoor (testing) scenes, object categories often change significantly, while the images’ visual domain is altered, such as under different lighting, weather conditions, *etc.*

To address this issue, in this work, we propose a new problem, namely open-domain open-vocabulary object detection (ODOV) to address the compound generalization of categories and domains, as shown in Figure 1. Specifically, during training, we learn the detection model *only on the base categories with the natural domain*. In testing, we expect the model can detect and classify *the objects with unseen categories and domains*. Clearly, this problem is more practical yet challenging, it faces two main new difficulties.

Problem divergence: Category and domain generalization typically operate under different mechanisms. While category generalization focuses on enhancing the model’s ability to recognize a diverse range of objects, domain generalization deals with adapting to variations in visual representation, such as changes in artistic style or environmental conditions. Striking a balance between these two objectives is difficult since improper integration may degrade the model’s overall performance.

Benchmark shortage: Existing object detection datasets with numerous categories, *e.g.*, LVIS, only contain the single-domain (natural) images. The open domain-related object detection datasets, *e.g.*, BDD100K [20], with several image styles, only involve specific object categories, *i.e.*, human and vehicle. Therefore, developing a benchmark with a compound of category and domain shifts is a principal requirement for this problem. Considering these two difficulties, we build a new benchmark and novel baseline methods, for ODOV object detection, aiming to encourage attention to and exploration of solutions to this critical setting.

With respect to the benchmark, we build a new evaluation dataset since our main purpose is to effectively test the algorithm ability for the ODOV object detection problem. Specifically, we designed the benchmark based on the LVIS validation set, named Open-Domain LVIS Benchmark (OD-LVIS). OD-LVIS comprises a total of 46,949 images and shares categories with LVIS, encompassing 1,203 categories across 18 diverse and complex real-world domains. It aims to provide a more comprehensive and useful testing dataset for ODOV object detection.

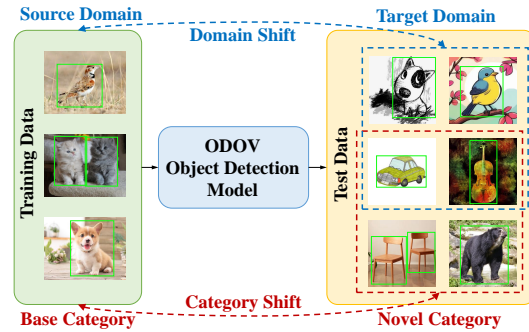


Figure 1: Illustration of ODOV object detection focusing on the simultaneous category shift and domain shift.

With respect to the method, we propose a novel method to enhance the model’s generalization capability for ODOV object detection. Our idea is to take full advantage of the large Vision-Language Models (VLMs) *e.g.*, CLIP [21], ALIGN [22], for enhancing the domain-guided information and category-aware prompts, for the domain and category generalization. Different from previous methods using VLMs for domain-generalized [23] or open-category [8, 24, 25, 26, 27, 28, 29, 9] object detection, a new difficulty in this work is to balance the concomitant category and domain shifts, as discussed above. To address it, we aim to make full use of the knowledge of original (frozen) CLIP, which has been learned on various object categories and image domains. For this purpose, we first utilize the large language models to generate the Domain-Agnostic Category Description as pure and detailed category Prompts (DAPmt). Next, we propose a Domain Projection and Grafting (DP&G) module to extract the *domain-specific embedding* of the input image, which is grafted to the *domain-agnostic category embedding* from DAPmt, to construct the customized prompting embedding for each given image, for effectively improving the ODOV object detection.

In summary, the main contributions of this work are:

- We propose a new problem of Open-Domain Open-Vocabulary (ODOV) object detection, which is designed to address the compound generalization of categories and domains in object detection. ODOV is more common and practical in many real-world scenarios.
- We construct a new benchmark for ODOV detection, OD-LVIS, which comprise over 46k images across 18 diverse real-world domains and 1,203 categories. OD-LVIS provides a comprehensive evaluation platform for open-scene detection models, which is available at OD-LVIS.
- We develop a novel ODOV detection framework. In this framework, we design the DAPmt module to generate the category-prominent but domain-agnostic category prompt, which is integrated with a domain-specific embedding from a novel domain projection and grafting (DP&G) module. During inference, this enables the model to detect the open-vocabulary-category objects while being adaptive to the given images’ open domains.

2 Related Work

Open-vocabulary object detection (OVD) [30] aims to detect objects from novel categories unseen during training. Leveraging the zero-shot capabilities of vision-language models (VLMs), recent advancements in OVD have emerged. Works like [31, 32, 33, 34, 35] use region-aware training to integrate image-text pairs, improving classification, especially for novel categories. Studies such as [36, 24, 37, 38, 39] use large-scale image-text data, pre-trained VLMs, or pseudo-labels to predict novel categories and fine-tune the model with both pseudo and base labels. Other methods [8, 40, 26, 29, 41, 9] employ knowledge distillation from VLMs to achieve OVD, transferring knowledge while enhancing localization. Some approaches build detectors on frozen VLMs [27, 25, 42], avoiding knowledge loss in fine-tuning and maximizing generalization. In this work, we use frozen VLMs as encoders, exploring their potential for category and domain generalization through prompt adjustment, revealing their strengths in open-domain and open-vocabulary object detection.

Domain Generalization (DG) based object detection aims to train a detector on multiple source domains to generalize to unseen target domains. Early work [11] used feature disentanglement for cross-domain generalization, followed by the Gated Disentangling Network [12], which activates feature channels for domain-invariant aspects. However, these methods rely on multiple domains and domain labels. Single Domain Generalized (SDG) object detection [13] addresses training with only one source domain. CDSO [13] separates domain-invariant from domain-specific representations, CLIP the Gap [14] uses pre-trained VLM, SRCD [15] reduces spurious correlations, and G-NAS [16] introduces a generalization loss to prevent Neural Architecture Search (NAS) overfitting. In this work, we adopt the SDG setting, using single-source domain data for training and evaluating multiple open domains. Our benchmark includes 18 diverse open domains, providing a more complex testbed than prior works.

Prompt learning for VLM adaptation. VLMs [21, 22, 43, 44, 45, 46] bridge image and text effectively. Pretrained on vast image-text pairs, models like CLIP [21] and ALIGN [22] excel in open-scene recognition. However, adapting them to specific tasks with limited data is challenging. Text prompts guide VLMs, but even advanced prompt learning methods [47, 48, 49] still require

training data. Recently, test-time prompt tuning (TPT) [50] creates prompts during testing through consistency regularization, though it struggles with distribution shifts. Our work explores VLM adaptation for open-domain and open-vocabulary settings at test time. By fusing style features with category descriptors, we dynamically create task-relevant embeddings, enhancing generalization across new categories and domains. Unlike traditional test-time prompt tuning (e.g., TPT), our approach directly addresses distribution shifts, significantly improving model generalization across both categories and domains.

3 ODOV Object Detection Benchmark

3.1 Problem Formulation

We first provide the problem formulation of the proposed ODOV object detection problem. During the training stage, we use the data from the *single source domain* (i.e., the natural image domain). Specifically, the training image dataset is notated as $\mathcal{D}^{\text{train}} = \{\mathbf{I}_i^{\text{train}}, L_i\}_{i=1}^N$, where N is the number of training images, \mathbf{I}_i denotes an image from the source domain with the detection annotation L_i for it. The label L_i is composed of $\{\mathbf{b}_i, \mathbf{c}_i\}$, in which \mathbf{b}_i indicates all the annotated object bounding boxes in \mathbf{I}_i , and the corresponding object categories are stored in \mathbf{c}_i . Note that, all the (annotated) object categories contained in L_i of the training set $\mathcal{D}^{\text{train}}$ are from the *base category* set, i.e., $\mathcal{C}^{\text{base}}$.

During the testing stage, the ODOV detection task requires the model to be applied under open-domain conditions as well as open-vocabulary conditions. Specifically, the testing images are from hybrid open domains (e.g., with various image styles), which are denoted as $\mathcal{D}^{\text{test}} = \{\mathbf{I}_j^{\text{test}}\}_{j=1}^M$ and M is the dataset scale. For each test image $\mathbf{I}_j^{\text{test}}$, the desired output is the predicted object bounding boxes with corresponding categories, i.e., $\{\mathbf{b}_j, \mathbf{c}_j\}$. Note that, following the open-vocabulary detection setting, the predicted objects contain both the base categories $\mathcal{C}^{\text{base}}$ (appearing in training) and the *novel categories* $\mathcal{C}^{\text{novel}}$ (unseen during training), which are combined as the open-vocabulary category set, i.e., $\mathcal{C}^{\text{open}} = \mathcal{C}^{\text{base}} + \mathcal{C}^{\text{novel}}$.

3.2 Motivation and Principles

As shown in Table 1, we summarize existing object detection datasets as follows. 1) *General-category detection*: Clipart [56], Watercolor [56], Comic [56], and MSOSB [62], with artistic styles; MS COCO [51], Objects365 [59], ODinW [61] and LVIS [60] consisting of common images with LVIS offering a more extensive set of categories often used for OV tasks. 2) *Specific-category detection*: WIDER FACE [54], a dataset representing common photographic scenes, focused solely on the face category. Besides, pedestrian detection and vehicle detection are also very popular with a series of datasets [63, 64, 65], etc. 3) *Traffic scene detection*: Cityscapes [52], BDD100K [20], Foggy Cityscapes [55], UFDD [57], RTTS [58], and Sim10K [53] contain unique weather conditions to test the domain generalization performance of models, but primarily focus on a limited set of objects common in traffic scenarios. Overall, the above **existing datasets do not meet the requirement of containing simultaneous open-domain and open-category scenes**.

Table 1: Comparison of OD-LVIS and other detection datasets.

Name	# Image	# Category	# Domains	# Domain Type
MS COCO (val) [51]	5,000	80	1	Normal
Cityscapes [52]	3,475	8	1	Weather
Sim10K [53]	10,000	1	1	Weather
WIDER FACE [54]	32,000	1	1	Normal
Foggy Cityscapes [55]	3,475	8	1	Weather
Clipart [56]	1,000	20	1	Art
Watercolor [56]	1,905	6	1	Art
Comic [56]	1,905	6	1	Art
UFDD [57]	884	1	1	Normal
RTTS [58]	9,109	5	1	Weather
Objects365 [59]	100,000	365	1	Normal
LVIS (val) [60]	19,809	1,203	1	Normal
BDD100K [20]	41,986	10	12	Weather
ODinW [61]	20,000	314	1	Normal
MSOSB [62]	76,146	80	5	Art
OD-LVIS	46,949	1,203	18	Art, Weather, Noise, Blur...

This way, we build OD-LVIS, a dedicated evaluation benchmark designed specifically for ODOV object detection, encompassing a diverse range of categories and complex real-world scenarios. Specifically, we select the LVIS as our basic dataset. On one hand, we inherit all the object categories in LVIS to guarantee the benchmark’s category diversity. On the other hand, to enhance the domain diversity, we extend the data by considering two aspects, i.e., the *image styles* and the *imaging conditions*. Specifically, for the former, we collect nine distinct styles, i.e., black-and-white pencil sketches, color pencil sketches, oil paintings, cartoons, watercolors, symbolism, impressionism,

gothic art, and lyrical abstraction. For the latter, we also consider nine imaging conditions, *i.e.*, rain, haze, illumination variations, low resolution, Gaussian white noise, Gaussian blur, salt-and-pepper noise, motion blur, and out-of-focus. As a result, OD-LVIS comprises 46,949 images across 18 different real-world domains, shares categories with LVIS, and adheres to its annotation guidelines, establishing a standardized benchmark for ODOV object detection evaluation.

3.3 Data Generation, Cleaning and Annotation

Collection During the construction of OD-LVIS, we first sampled images from the LVIS validation set for each open domain, ensuring coverage of all categories, and then applied domain transformation processing to generate the open-domain data. In total, we design 18 open domains, including nine types of imaging conditions and nine image styles.

Open-domain generation for various imaging conditions. We generate images with nine types of imaging conditions from clear images to enhance the domain diversity. The specific methods are as follows: ① *Rainy Images*: Leveraging [66], we created diverse rainy scene images to enrich the dataset’s representation of rain scenarios. ② *Hazy Images*: Following [67], we synthesized hazy images with varying concentrations by altering the atmospheric scattering coefficient. ③ *Illumination Variations*: Illumination conditions were diversified using gamma correction, with different gamma values applied to adjust the lighting. ④ *Low Resolution*: Based on [68, 69], high-resolution images were downsampled using a bicubic kernel, with the degradation level controlled by the downsampling factor. ⑤ *Gaussian White Noise*: Inspired by [70], we synthesized Gaussian white noise images with varying degradation levels by modifying the noise variance. ⑥ *Gaussian Blur*: Following [71], we added Gaussian blur with degradation intensity controlled by Gaussian kernel standard deviation. ⑦ *Salt-and-Pepper Noise*: Similarly, we added salt-and-pepper noise with degradation intensity controlled by noise density [71]. ⑧ *Motion Blur*: Following [72], we synthesized images with varying degrees of motion blur by adjusting the blur kernel length. ⑨ *Out-of-focus*: Using the method from [73], we generated defocused images by adjusting the radius of a circular averaging filter.

Open-domain generation for various image styles. We also generate images with nine types of image styles to further enrich the dataset’s diversity. Specifically, we use Baidu’s Style Transfer API, to generate images with nine image styles, including pencil sketches, watercolors, *etc.* These styles of images are very common on the Internet, especially with the rapid expansion of generative artificial intelligence. The generated image provides more diverse and challenging data for open-domain object detection tasks.

Cleaning and annotation. Upon completing data generation, we established strict image selection criteria to ensure the benchmark’s quality. Specifically, to ensure the reliability of the selection process, we enlisted several related researchers for participation and supervision. The manual selection is required to ensure that the images and objects remain clear, the content is intact, and object categories are easily identifiable. Since the generation was conducted based on the LVIS, we were able to retain the original annotations, including both object detection and instance segmentation labels. Note that, the domain amplification of OD-LVIS *has no impact* on the object annotations of LVIS since no resizing or deformation of the objects occurred during synthesis. Finally, we organized the annotations and standardized them into VOC and LVIS formats. It is worth to mention that, since OD-LVIS shares categories with LVIS, it can be combined with LVIS (used for training) to further assess the domain generalization ability of object detection models across 18 various scenes.

3.4 Preliminary Experiments on OD-LVIS

We investigate the impact of OD-LVIS on existing detector. Take the haze and noise for example, we evaluate the SOTA OVD method CLIPSelf (ViT-B/16) [9] in Table 2, where m and k control the levels of haze and noise, respectively (larger values indicate more severe shifts). Results show that as domain shifts increase, model performance declines significantly, demonstrating the necessity of the studying on ODOV detection and OD-LVIS benchmark. In the *supplementary materials*, we present more details and example images of various conditions/styles in OD-LVIS.

Table 2: Results on images with varying degrees of degradation.

Data	Degree / AP (%)	Degree / AP (%)
Source	- / 26.2	- / 26.2
Haze	$m=0.05$ / 24.2	$m=0.08$ / 20.6
Noise	$k=0.04$ / 13.6	$k=0.06$ / 12.9

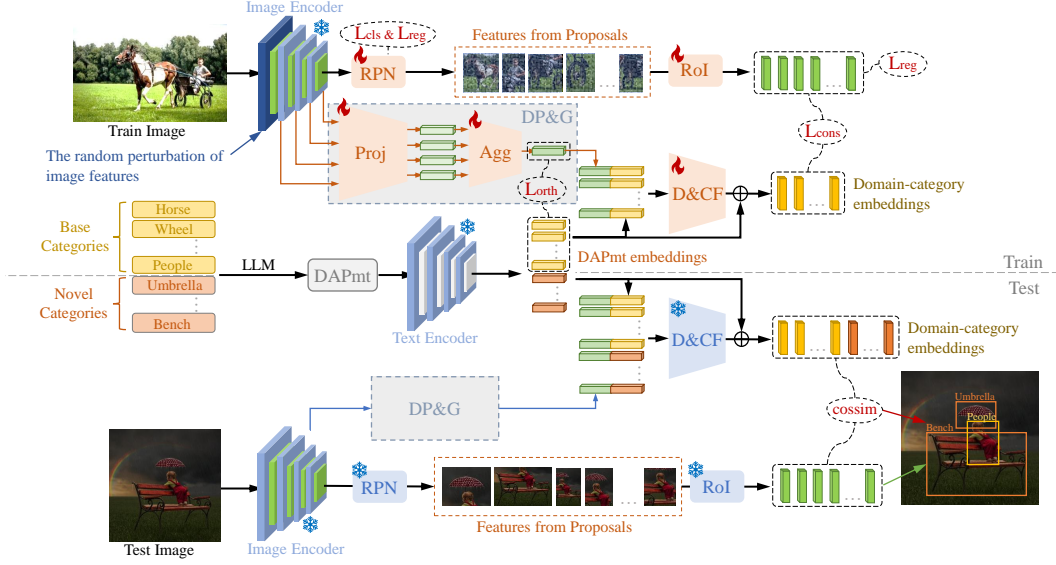


Figure 2: Illustration of our method. We leverage the generalization capabilities of pre-trained vision-language models (CLIP) by decoupling domain-aware representations and recombining them with domain-agnostic category embeddings to adapt to the ODOV detection task.

4 The Proposed Baseline Method

4.1 Overview

We aim to leverage the generalization capabilities of pre-trained VLMs, *e.g.* CLIP, to address the alignment challenge between image and prompt embeddings in ODOV object detection. As illustrated in Figure 2, we employ frozen CLIP encoders and propose a customized prompt embedding strategy that accounts for both category diversity and domain variations. Specifically, we learn the *Domain-Agnostic Category Prompt (DAPmt)* to capture the core semantics of each category, and design a learnable *Domain Projection and Grafting (DP&G)* network to integrate domain-specific features from images into the DAPmt. Since training images come from a single source domain, we adopt implicit domain augmentation and contrastive learning to align image and prompt embeddings during training. In testing, the fused embeddings are dynamically generated based on the domain characteristics of each image, enabling robust recognition of novel categories across diverse domains.

4.2 Domain-Agnostic Category Prompt (DAPmt)

VLMs such as CLIP associate the visual images with text captions through large-scale pre-training. CLIP based open-scene detection has achieved high accuracy on multiple datasets, utilizing the manually crafted prompts (*e.g.*, ‘a photo of { }’) as the text prompts. Such simple prompts are easy to obtain, but can not make full use of the VLMs, which is especially highlighted in the OSOV setting since the same category of object from different domains shows various characteristics. Some recent works [8, 24, 27, 9, 26] manually design the prompt templates considering the dataset characteristics. For example, using templates like ‘a black-and-white photo of { }’ or ‘a rainy photo of { }’, which are time-consuming and also difficult to generalize to other datasets.

Although various learnable and automated prompt generation methods [74, 75, 76, 77, 78] have been proposed, they typically rely on generic category descriptions, overlooking the representation of category-specific attributes and the disentanglement of style information, as their focus remains on conventional OVD tasks.

To overcome these challenges and obtain prompts to identify the categories across diverse open domains, we propose a prompting method using large language models (LLMs). Specifically, we leverage LLMs to generate category-specific but domain-agnostic attribute descriptions for each category in the dataset, as the Domain-Agnostic Category Prompt (DAPmt). Through the LLM, we aim to create detailed text descriptions for each category, allowing them to *incorporate fine-grained details that differentiate other similar categories but are not impacted by specific domains*.

For this purpose, we utilize the LLM, namely ChatGPT-4o, to generate the DAPmt. For each category, we provide ChatGPT-4o with an instruction template in the form of ‘A/An {category} has/is [Appearance feature1], [Appearance feature2], ...’. During the generation, we manually instruct ChatGPT-4o to ensure that [Appearance feature] elements within each category are not repetitive, emphasizing the particular visual representations for each category and remaining consistent across different domains (*e.g.*, ignoring style information). For example, we generate the description for {Airplane}: ‘An airplane is a large vehicle with long wings and a streamlined body’. This way, the generated descriptions are robust and adaptable to varying styles and backgrounds for the same category. Additionally, to prevent domain-dependent color features (easily be influenced by illumination, artistic style, *etc*), we avoid color-related attributes. Although this method requires some manual adjustments, it is considerably less labor-intensive than traditional manually designed prompt engineering, which often relies on extensive handcrafted sentences. Overall, our strategy focuses on generating domain-agnostic prompts to guide the model toward a general but accurate understanding of each category, thereby improving robustness in ODOV problems.

As discussed above, we design the DAPmt, which contains more detailed descriptions but less domain-aware information, for each category. Next, to handle the open-domain problem, we propose a domain projection and grafting strategy. Our basic idea is that, for each given image (to be detected), we aim to leverage the domain-aware embedding reflecting its domain characteristic, *i.e.*, image styles, imaging conditions, *etc*. For the detection task, we aim to get the *customized embedding*, which encodes domain embedding containing the specific domain information from the input image itself, and the text embeddings from the above category DAPmt. Next, we discuss domain-aware embedding projection and grafting strategy.

4.3 Domain Projection and Grafting (DP&G)

Next, we discuss how to effectively leverage the domain information of each given image through our *Domain Projection and Grafting (DP&G)* module.

Domain-aware embedding extraction. First, we extract the multi-level domain-aware features. Specifically, during training on single source-domain data, we first apply random perturbations to the features based on the classic AdaIN [79] and NP [10] methods to simulate domain variations¹. Then, for an input image \mathbf{I} , we extract the (disturbed) feature map $\mathbf{F}_l \in \mathbb{R}^{W \times H \times C}$ from the l^{th} layer of the image encoder \mathcal{E} , in which W, H, C denote the height, width, and channel, respectively. For the c^{th} channel, the mean μ_l^c and standard deviation σ_l^c are computed as $\mu_l^c = \text{avg}(\mathbf{F}_l^c(w, h)), \sigma_l^c = \sqrt{\text{avg}(\mathbf{F}_l^c(w, h) - \mu_l^c)^2}$. We contact all C channels of μ_l^c and σ_l^c to obtain the mean/standard deviation vectors, as $\mu_l \in \mathbb{R}^C$ and $\sigma_l \in \mathbb{R}^C$. This way, we can obtain the initial domain-aware features by concatenating the mean and standard deviation vectors as $\mathcal{E}_l = [\mu_l; \sigma_l]$.

The domain feature of layer l namely \mathcal{E}_l is then processed through adaptive average pooling and a fully connected layer to align the dimension with that of the DAPmt embeddings (Section 4.2). As shown in Figure 2, we extract the domain features from multiple layers. These features are then input into an aggregation network to get the final domain embedding $\mathbf{E}_{\text{domain}}$, in which a set of learnable weights dynamically balances the contributions from each layer through weighted integration.

Orthogonality constraint for embedding alignment. We then consider to project the domain embedding $\mathbf{E}_{\text{domain}}$ into a regularized embedding space. Specifically, we hope the learned domain-aware embeddings are *irrelevant* (orthometric) to the category embedding. For this purpose, we apply an orthogonality constraint loss, which minimizes the similarity between the domain embeddings and the category DAPmt embeddings, thereby effectively separating them, as $\mathcal{L}_{\text{orth}} = \sum_{g=1}^{C^{\text{base}}} \text{cossim}(\mathbf{E}_{\text{domain}}, \mathbf{E}_{\text{category}}^g)$, where $\mathbf{E}_{\text{domain}}$ represents the learnable domain embedding, $\mathbf{E}_{\text{category}}^g$ denotes the DAPmt embedding for the g^{th} category, C^{base} is the total number of (base) categories, and cossim denotes the cosine similarity.

Grafting the domain-specific embedding to DAPmt. Finally, we develop a domain and category embedding fusion (D&CF) network. Specifically, we concatenate the domain and category embeddings, followed by a multi-layer perceptron (MLP) to project it into the fusion space as $\mathbf{E}_{\text{fusion}}^g = \text{MLP}([\mathbf{E}_{\text{domain}}; \mathbf{E}_{\text{category}}^g])$, which denotes the fused embedding for the g -th category.

¹Following the rationale in [79], the mean and standard deviation in the feature map implicitly represent the domain-aware information.

After that, to preserve core semantic information from the category text descriptions, a residual connection of $\mathbf{E}_{\text{category}}^g$ is applied as $\mathbf{E}_{\text{D\&CF}}^g = \alpha \cdot \mathbf{E}_{\text{fusion}}^g + (1 - \alpha) \cdot \mathbf{E}_{\text{category}}^g$, where a learnable parameter α within the range $[0, 1]$ is used to dynamically balance the direct fusion embedding and the original category embedding $\mathbf{E}_{\text{category}}^g$.

After the D&CF network, the proposed method grafts the domain-specific embedding (from the input image) on the domain-agnostic category embedding (from DAPmt), to generate the *customized domain-category embeddings for each given image and category prompt*, thereby improving the ODOV detection ability.

Finally, during training, we extract the visual features (with added disturbance) from the image encoder as \mathbf{F}_I , and we use the ROI Align [80] to obtain the object-level visual features as \mathbf{F}_{RoI} . Then we use the contrastive loss to align the above domain-category embedding $\mathbf{E}_{\text{D\&CF}}^g$ with \mathbf{F}_{RoI} as $\mathcal{L}_{\text{cons}} = 1 - \frac{\mathbf{E}_{\text{D\&CF}}^g \cdot \mathbf{F}_{\text{RoI}}}{\|\mathbf{E}_{\text{D\&CF}}^g\| \|\mathbf{F}_{\text{RoI}}\|}$, where $\|\cdot\|$ is the L_2 norm of a vector.

4.4 Implementation Details

Training stage. During training, we apply random perturbations to the mean and standard deviation of the first and second layer features output by the image encoder, and simultaneously, the multi-layer domain features in DP&G are drawn from layers [3, 5, 7, 11] of ViT-B/16, layers [6, 10, 14, 23] of ViT-L/14, and all layers of ResNet. Our method is trained using 16 3090 GPUs, with a batchsize of 10 per GPU. We use AdamW configured with a learning rate of 10^{-4} and a weight decay of 0.1. Training is conducted on the LVIS training set for 50 epochs.

Testing stage. During testing, the images come from diverse open domains so we do not apply the random perturbations on the features for simulative domain argumentation. Similar to the training phase, we use the trained DP&G network to extract domain information to generate domain embeddings, which is fused with the DAPmt embeddings for both *base and novel* categories. Finally, the RPN-extracted proposals are used for bounding box localization, and cosine similarity with the domain-category fused embeddings is calculated for object classification.

5 Experimental Results

5.1 Setup

ODOV settings. For the open domain, we train the models on single-domain natural images (LVIS training set) and test on all 18 open-domains in OD-LVIS, similar to the single-domain generalization setting [81]. For the open vocabulary, we follow the OVD approach ViLD [8] for dataset splitting. Among all categories in OD-LVIS, *i.e.*, in LVIS [60], 405 ‘frequent’ and 461 ‘common’ categories are assigned as base categories for training, while 337 ‘rare’ categories are novel categories only for testing. Note that, OD-LVIS is the *only benchmark meeting the ODOV setting*, so all main experiments are conducted on it.

Evaluation methods. To build the benchmark evaluation of the ODOV detection, we selected several mainstream VLM-based OVD methods for comparison on OD-LVIS. Specifically, we include the transfer learning approaches, *i.e.*, F-VLM [27], OWL-ViT [25], CLIPSelf [9], MM-OVOD [28], and OV-DQUO [42], and several knowledge distillation methods, *i.e.*, RKDWTF [26], DK-DETR [29], RegionCLIP [24], and region-aware training method YOLO-World [82]. We also include two recent domain generalization (DG) methods, ALT [83] and ABA [84], for comparison.

Evaluation metrics. For the evaluation metrics, the average precision on ‘frequent’ and ‘common’ categories, denoted as AP_f and AP_c , respectively, serves as the metric for base categories, while the average precision on ‘rare’ categories, denoted as AP_r , is used to evaluate novel categories. The average precision for all categories is denoted as AP .

5.2 Main Results on OD-LVIS

Table 3 shows the results of all comparative methods and ours on OD-LVIS. We can first see that, the proposed method (Ours w ViT-L/14) with the DAPmt and DP&G modules, achieves the best performance among all competitors. Specifically, with the ViT-L/14 (model size of 304.43M), ‘Ours’ achieves improvements of 1.4%, 1.6%, 1.4%, and 1.5% (‘frequent’, ‘common’, ‘rare’, and overall

Table 3: Comparison with SOTA on OD-LVIS (%).

Method	Backbone	AP_f	AP_c	AP_r	AP
RegionCLIP [24]	RN50	16.6	13.0	9.7	13.9
RegionCLIP	RN50x4	19.5	15.8	12.4	16.7
OWL-ViT [25]	ViT-B/16	13.1	13.9	13.2	13.5
OWL-ViT	ViT-L/14	22.1	21.6	19.9	21.5
RKDWTF [26]	RN50 Base	14.6	12.4	8.7	12.6
RKDWTF	RN50 RKDPIS	13.4	12.1	10.3	12.3
RKDWTF	RN50 WTF	14.0	12.5	11.3	12.9
RKDWTF	RN50 WTF8x	15.8	14.3	11.9	14.5
MM-OVOD [28]	RN50_Avg	20.3	19.2	14.1	18.8
MM-OVOD	RN50_Agg	20.5	19.8	14.0	19.0
MM-OVOD+DAPmt	RN50_Agg	20.8	20.4	14.5	19.5
MM-OVOD	RN50_Avg_in-L	20.2	19.8	16.1	19.4
MM-OVOD	RN50_Agg_in-L	20.4	20.4	15.9	19.6
DK-DETR [29]	RN50	21.1	19.4	15.3	19.4
YOLO-World-L [82]	YOLOv8-L	21.9	19.1	19.3	20.2
YOLO-World-L+DAPmt	YOLOv8-L	22.0	19.6	19.7	20.6
F-VLM [27]	RN50	15.1	12.2	9.9	12.9
F-VLM	RN50x4	15.8	12.9	11.7	13.8
F-VLM	RN50x16	16.7	14.4	13.7	15.2
F-VLM	RN50x64	18.1	16.6	15.1	16.9
OV-DQUO [42]	ViT-B/16	12.8	14.8	14.8	14.0
OV-DQUO+DAPmt	ViT-B/16	13.1	15.0	15.3	14.3
OV-DQUO	ViT-L/14	16.4	20.6	21.2	19.1
ClipSelf [9]	ViT-B/16	17.1	12.0	12.2	14.0
ClipSelf	ViT-L/14	22.5	21.3	20.2	21.6
DAPmt	RN50x16	17.2	15.3	14.7	16.0
DP&G		17.5	16.2	15.2	16.5
Ours (DAPmt + DP&G)		17.6	16.9	15.8	17.0
DAPmt	ViT-B/16	17.5	12.7	13.2	14.7
DP&G		18.6	13.8	13.7	15.7
Ours (DAPmt + DP&G)		19.0	14.3	14.0	16.1
DAPmt	ViT-L/14	22.8	21.7	20.8	22.0
DP&G		23.5	22.2	21.5	22.6
Ours (DAPmt + DP&G)		23.9	22.9	21.6	23.1

categories) over CLIPSelf with the same backbone. For smaller networks, ViT-B/16 (86.26M) or RN50x16 (167.33M), compared to CLIPSelf or F-VLM using the same backbone, the achievements reach 2.1% and 1.8%, respectively on overall AP . Ours with RN50x16 (17.0% @ AP) even outperforms the F-VLM using a much larger backbone of RN50x64 (16.9% @ AP). These results verify the significant advantage of the DAPmt and DP&G modules supporting improved generalization in open-domain detection. Moreover, from the results of all methods, we also find that the performance on OD-LVIS is generally low, which demonstrates that this benchmark is challenging, with much room for improvement. In Appendix 7, we present additional comparison results of our method on LVIS, along with performance comparisons against SOTA DG methods on OD-LVIS. We also provide visualization results on images with varying styles.

5.3 Ablation Study

Effectiveness of the proposed DAPmt. As shown in Table 3, when using ViT-B/16 as the backbone, with only using DAPmt module in our method, our methods ‘DAPmt’ achieves the scores of 17.5%, 12.7%, 13.2%, and 14.7% for the ‘frequent’, ‘common’, ‘rare’, and overall categories, which outperforms CLIPSelf for 0.4%, 0.7%, 1.0%, and 0.7%. The results of using the ViT-L/14 or ResNet as the backbone are similar. These results indicate that introducing DAPmt in the training process enables our model to effectively learn the category semantics from CLIP, thus enhancing the model’s generalization capabilities.

Effectiveness of the proposed DP&G. To validate the DP&G solely, we train DP&G based on fixed prompt templates (e.g., ‘a photo of { }’) instead of using DAPmt. The corresponding results ‘DP&G’ show that, with the ViT-B/16 backbone, it achieves the improvements of 1.5%, 1.8%, 1.5%, and 1.7% for ‘frequent’, ‘common’, ‘rare’, and overall categories over CLIPSelf. We can also see the improvements when using the ViT-L/14 backbone and ResNet. We attribute this to DP&G’s ability to extract and incorporate the visual domain information, enriching representation of the customized prompts, thereby enhancing the model’s generalization across diverse scenarios. When comparing the only ‘DAPmt’ or ‘DP&G’ with ‘Ours’ (DAPmt + DP&G), it can also be seen that removing either of them decreases the performance of our method, which verifies the effectiveness of both.

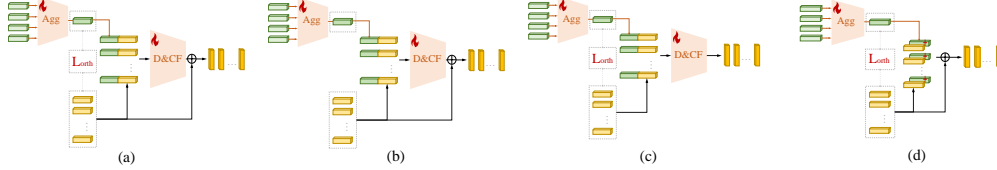


Figure 3: Ablation study of different fusion structures.

Ablation study of different structures. As shown in Figure 3, we compare: (a) Ours; (b) Removing the orthogonal regularization loss; (c) Removing the residual connection; (d) Replacing the D&CF module with a direct weighted summation. As shown in Table 4, the structure in (b) results in an overall performance drop. This is because the domain embeddings extracted from the input images may still contain a small amount of object category information, and without maintaining orthogonality, the fusion text features contain reduced category discrimination than the original, which negatively impacts the model’s recognition accuracy. Structure (c) leads to a significant drop in accuracy for novel categories, indicating that the fusion process may cause some semantic information of categories to be lost. This indicates that the residual connection helps retain original semantic information, thus enhancing the model’s generalization capability for novel categories. Structure (d) also causes an accuracy drop. This direct fusion method is too simplistic to effectively integrate the two feature types, resulting in suboptimal performance.

Table 4: Ablation study of the fusion process on OD-LVIS (%).

Struct.	AP_f	AP_c	AP_r	AP
(a)	19.0	14.3	14.0	16.1
(b)	18.6	14.0	12.9	15.6
(c)	18.4	13.8	8.9	14.8
(d)	17.9	12.7	12.4	14.7

6 Conclusion

We have proposed to study a new yet practical problem of ODOV object detection, by considering both the domain and category shifts. For this purpose, we construct the benchmark OD-LVIS containing 18 domains and 1,203 categories. We have also developed a baseline method for ODOV detection, which can generate the domain-agnostic text prompts for category embedding, as well as the domain embeddings using a domain projection and grafting network. By combining both of them, we obtain the customized domain-specific category embedding for each test image, which well adapts ODOV detection. We provide the benchmark evaluation of a series of SOTA methods on OD-LVIS. Through these efforts, we hope to pave the way for the study of this new yet significant problem.

References

- [1] Ting-I Hsieh, Yi-Chen Lo, Hwann-Tzong Chen, and Tyng-Luh Liu. One-shot object detection with co-attention and co-excitation. *Advances in neural information processing systems*, 32:1–10, 2019.
- [2] Ding-Jie Chen, He-Yen Hsieh, and Tyng-Luh Liu. Adaptive image transformer for one-shot object detection. In *Proceedings of the IEEE/CVF Conference on Computer Vision and Pattern Recognition*, pages 12247–12256, 2021.
- [3] Yizhou Zhao, Xun Guo, and Yan Lu. Semantic-aligned fusion transformer for one-shot object detection. In *Proceedings of the IEEE/CVF Conference on Computer Vision and Pattern Recognition*, pages 7601–7611, 2022.
- [4] Hanqing Yang, Sijia Cai, Hualian Sheng, Bing Deng, Jianqiang Huang, Xian-Sheng Hua, Yong Tang, and Yu Zhang. Balanced and hierarchical relation learning for one-shot object detection. In *Proceedings of the IEEE/CVF Conference on Computer Vision and Pattern Recognition*, pages 7591–7600, 2022.

- [5] Zhenyu Wang, Yali Li, Xi Chen, Ser-Nam Lim, Antonio Torralba, Hengshuang Zhao, and Shengjin Wang. Detecting everything in the open world: Towards universal object detection. In *Proceedings of the IEEE/CVF Conference on Computer Vision and Pattern Recognition*, pages 11433–11443, 2023.
- [6] Zeyu Ma, Yang Yang, Guoqing Wang, Xing Xu, Heng Tao Shen, and Mingxing Zhang. Rethinking open-world object detection in autonomous driving scenarios. In *Proceedings of the 30th ACM International Conference on Multimedia*, pages 1279–1288, 2022.
- [7] Sahal Shaji Mullappilly, Abhishek Singh Gehlot, Rao Muhammad Anwer, Fahad Shahbaz Khan, and Hisham Cholakkal. Semi-supervised open-world object detection. In *Proceedings of the AAAI Conference on Artificial Intelligence*, volume 38, pages 4305–4314, 2024.
- [8] Xiuye Gu, Tsung-Yi Lin, Weicheng Kuo, and Yin Cui. Open-vocabulary object detection via vision and language knowledge distillation. *arXiv preprint arXiv:2104.13921*, 2021.
- [9] Size Wu, Wenwei Zhang, Lumin Xu, Sheng Jin, Xiangtai Li, Wentao Liu, and Chen Change Loy. Clipself: Vision transformer distills itself for open-vocabulary dense prediction. *arXiv preprint arXiv:2310.01403*, 2023.
- [10] Qi Fan, Mattia Segu, Yu-Wing Tai, Fisher Yu, Chi-Keung Tang, Bernt Schiele, and Dengxin Dai. Towards robust object detection invariant to real-world domain shifts. In *The Eleventh International Conference on Learning Representations (ICLR 2023)*, 2023.
- [11] Chuang Lin, Zehuan Yuan, Sicheng Zhao, Peize Sun, Changhu Wang, and Jianfei Cai. Domain-invariant disentangled network for generalizable object detection. In *Proceedings of the IEEE/CVF international conference on computer vision*, pages 8771–8780, 2021.
- [12] Haozhuo Zhang, Huimin Yu, Yuming Yan, and Runfa Wang. Gated domain-invariant feature disentanglement for domain generalizable object detection. *arXiv preprint arXiv:2203.11432*, 2022.
- [13] Aming Wu and Cheng Deng. Single-domain generalized object detection in urban scene via cyclic-disentangled self-distillation. In *Proceedings of the IEEE/CVF Conference on computer vision and pattern recognition*, pages 847–856, 2022.
- [14] Vedit Vidit, Martin Engilberge, and Mathieu Salzmann. Clip the gap: A single domain generalization approach for object detection. In *Proceedings of the IEEE/CVF conference on computer vision and pattern recognition*, pages 3219–3229, 2023.
- [15] Zhijie Rao, Jingcai Guo, Luyao Tang, Yue Huang, Xinghao Ding, and Song Guo. Srcd: Semantic reasoning with compound domains for single-domain generalized object detection. *arXiv preprint arXiv:2307.01750*, 2023.
- [16] Fan Wu, Jinling Gao, Lanqing Hong, Xinbing Wang, Chenghu Zhou, and Nanyang Ye. G-nas: Generalizable neural architecture search for single domain generalization object detection. In *Proceedings of the AAAI Conference on Artificial Intelligence*, volume 38, pages 5958–5966, 2024.
- [17] Yongzhen Wang, Xuefeng Yan, Kaiwen Zhang, Lina Gong, Haoran Xie, Fu Lee Wang, and Mingqiang Wei. Togethernet: Bridging image restoration and object detection together via dynamic enhancement learning. In *Computer Graphics Forum*, volume 41, pages 465–476, 2022.
- [18] Jing Wang, Meimei Xu, Huazhu Xue, Zhanqiang Huo, and Fen Luo. Joint image restoration for object detection in snowy weather. *IET Computer Vision*, 2024.
- [19] Xiaofeng Wang, Xiao Liu, Hong Yang, Zhengyong Wang, Xiaoyue Wen, Xiaohai He, Linbo Qing, and Honggang Chen. Degradation modeling for restoration-enhanced object detection in adverse weather scenes. *IEEE Transactions on Intelligent Vehicles*, 2024.
- [20] Fisher Yu, Haofeng Chen, Xin Wang, Wenqi Xian, Yingying Chen, Fangchen Liu, Vashisht Madhavan, and Trevor Darrell. Bdd100k: A diverse driving dataset for heterogeneous multitask learning. In *Proceedings of the IEEE/CVF conference on computer vision and pattern recognition*, pages 2636–2645, 2020.
- [21] Alec Radford, Jong Wook Kim, Chris Hallacy, Aditya Ramesh, Gabriel Goh, Sandhini Agarwal, Girish Sastry, Amanda Askell, Pamela Mishkin, Jack Clark, et al. Learning transferable visual models from natural language supervision. In *International conference on machine learning*, pages 8748–8763, 2021.
- [22] Chao Jia, Yinfei Yang, Ye Xia, Yi-Ting Chen, Zarana Parekh, Hieu Pham, Quoc Le, Yun-Hsuan Sung, Zhen Li, and Tom Duerig. Scaling up visual and vision-language representation learning with noisy text supervision. In *International conference on machine learning*, pages 4904–4916, 2021.

- [23] Yang Shu, Xingzhuo Guo, Jialong Wu, Ximei Wang, Jianmin Wang, and Mingsheng Long. Clipood: Generalizing clip to out-of-distributions. In *International Conference on Machine Learning*, pages 31716–31731, 2023.
- [24] Yiwu Zhong, Jianwei Yang, Pengchuan Zhang, Chunyuan Li, Noel Codella, Liunian Harold Li, Luowei Zhou, Xiyang Dai, Lu Yuan, Yin Li, et al. Regionclip: Region-based language-image pretraining. In *Proceedings of the IEEE/CVF conference on computer vision and pattern recognition*, pages 16793–16803, 2022.
- [25] M Minderer, A Gritsenko, A Stone, M Neumann, D Weissenborn, A Dosovitskiy, A Mahendran, A Arnab, M Dehghani, Z Shen, et al. Simple open-vocabulary object detection with vision transformers. *arXiv preprint arXiv:2205.06230*, 2, 2022.
- [26] Hanoona Bangalath, Muhammad Maaz, Muhammad Uzair Khattak, Salman H Khan, and Fahad Shahbaz Khan. Bridging the gap between object and image-level representations for open-vocabulary detection. *Advances in Neural Information Processing Systems*, 35:33781–33794, 2022.
- [27] Weicheng Kuo, Yin Cui, Xiuye Gu, AJ Piergiovanni, and Anelia Angelova. F-vlm: Open-vocabulary object detection upon frozen vision and language models. *arXiv preprint arXiv:2209.15639*, 2022.
- [28] Yifan Xu, Mengdan Zhang, Xiaoshan Yang, and Changsheng Xu. Exploring multi-modal contextual knowledge for open-vocabulary object detection. *arXiv preprint arXiv:2308.15846*, 2023.
- [29] Liangqi Li, Jiaxu Miao, Dahu Shi, Wenming Tan, Ye Ren, Yi Yang, and Shiliang Pu. Distilling detr with visual-linguistic knowledge for open-vocabulary object detection. In *Proceedings of the IEEE/CVF International Conference on Computer Vision*, pages 6501–6510, 2023.
- [30] Alireza Zareian, Kevin Dela Rosa, Derek Hao Hu, and Shih-Fu Chang. Open-vocabulary object detection using captions. In *Proceedings of the IEEE/CVF Conference on Computer Vision and Pattern Recognition*, pages 14393–14402, 2021.
- [31] Dahun Kim, Anelia Angelova, and Weicheng Kuo. Contrastive feature masking open-vocabulary vision transformer. In *Proceedings of the IEEE/CVF International Conference on Computer Vision*, pages 15602–15612, 2023.
- [32] Dahun Kim, Anelia Angelova, and Weicheng Kuo. Detection-oriented image-text pretraining for open-vocabulary detection. *arXiv preprint arXiv:2310.00161*, 2023.
- [33] Dahun Kim, Anelia Angelova, and Weicheng Kuo. Region-aware pretraining for open-vocabulary object detection with vision transformers. In *Proceedings of the IEEE/CVF conference on computer vision and pattern recognition*, pages 11144–11154, 2023.
- [34] Xiaoshi Wu, Feng Zhu, Rui Zhao, and Hongsheng Li. Cora: Adapting clip for open-vocabulary detection with region prompting and anchor pre-matching. In *Proceedings of the IEEE/CVF conference on computer vision and pattern recognition*, pages 7031–7040, 2023.
- [35] Hwanjun Song and Jihwan Bang. Prompt-guided transformers for end-to-end open-vocabulary object detection. *arXiv preprint arXiv:2303.14386*, 2023.
- [36] Xingyi Zhou, Rohit Girdhar, Armand Joulin, Philipp Krähenbühl, and Ishan Misra. Detecting twenty-thousand classes using image-level supervision. In *European Conference on Computer Vision*, pages 350–368, 2022.
- [37] Joonhyun Jeong, Geondo Park, Jayeon Yoo, Hyungsik Jung, and Heesu Kim. Proxydet: Synthesizing proxy novel classes via classwise mixup for open-vocabulary object detection. In *Proceedings of the AAAI Conference on Artificial Intelligence*, volume 38, pages 2462–2470, 2024.
- [38] Chuofan Ma, Yi Jiang, Xin Wen, Zehuan Yuan, and Xiaojuan Qi. Codet: Co-occurrence guided region-word alignment for open-vocabulary object detection. *Advances in neural information processing systems*, 36, 2024.
- [39] Prannay Kaul, Weidi Xie, and Andrew Zisserman. Multi-modal classifiers for open-vocabulary object detection. In *International Conference on Machine Learning*, pages 15946–15969, 2023.
- [40] Chau Pham, Truong Vu, and Khoi Nguyen. Lp-ovod: Open-vocabulary object detection by linear probing. In *Proceedings of the IEEE/CVF Winter Conference on Applications of Computer Vision*, pages 779–788, 2024.

- [41] Yu Du, Fangyun Wei, Zihe Zhang, Miaoqing Shi, Yue Gao, and Guoqi Li. Learning to prompt for open-vocabulary object detection with vision-language model. In *Proceedings of the IEEE/CVF Conference on Computer Vision and Pattern Recognition*, pages 14084–14093, 2022.
- [42] Junjie Wang, Bin Chen, Bin Kang, Yulin Li, Weizhi Xian, Yichi Chen, and Yong Xu. Open-vocabulary detr with denoising text query training and open-world unknown objects supervision. In *Proceedings of the AAAI Conference on Artificial Intelligence*, volume 39, pages 7762–7770, 2025.
- [43] Xiaohua Zhai, Xiao Wang, Basil Mustafa, Andreas Steiner, Daniel Keysers, Alexander Kolesnikov, and Lucas Beyer. Lit: Zero-shot transfer with locked-image text tuning. In *Proceedings of the IEEE/CVF conference on computer vision and pattern recognition*, pages 18123–18133, 2022.
- [44] Lewei Yao, Runhui Huang, Lu Hou, Guansong Lu, Minzhe Niu, Hang Xu, Xiaodan Liang, Zhenguo Li, Xin Jiang, and Chunjing Xu. Filip: Fine-grained interactive language-image pre-training. *arXiv preprint arXiv:2111.07783*, 2021.
- [45] Lu Yuan, Dongdong Chen, Yi-Ling Chen, Noel Codella, Xiyang Dai, Jianfeng Gao, Houdong Hu, Xuedong Huang, Boxin Li, Chunyuan Li, et al. Florence: A new foundation model for computer vision. *arXiv preprint arXiv:2111.11432*, 2021.
- [46] Quan Sun, Yuxin Fang, Ledell Wu, Xinlong Wang, and Yue Cao. Eva-clip: Improved training techniques for clip at scale. *arXiv preprint arXiv:2303.15389*, 2023.
- [47] Kaiyang Zhou, Jingkang Yang, Chen Change Loy, and Ziwei Liu. Learning to prompt for vision-language models. *International Journal of Computer Vision*, 130(9):2337–2348, 2022.
- [48] Kaiyang Zhou, Jingkang Yang, Chen Change Loy, and Ziwei Liu. Conditional prompt learning for vision-language models. In *Proceedings of the IEEE/CVF conference on computer vision and pattern recognition*, pages 16816–16825, 2022.
- [49] Muhammad Uzair Khattak, Hanoona Rasheed, Muhammad Maaz, Salman Khan, and Fahad Shahbaz Khan. Maple: Multi-modal prompt learning. In *Proceedings of the IEEE/CVF Conference on Computer Vision and Pattern Recognition*, pages 19113–19122, 2023.
- [50] Manli Shu, Weili Nie, De-An Huang, Zhiding Yu, Tom Goldstein, Anima Anandkumar, and Chaowei Xiao. Test-time prompt tuning for zero-shot generalization in vision-language models. *Advances in Neural Information Processing Systems*, 35:14274–14289, 2022.
- [51] Tsung-Yi Lin, Michael Maire, Serge Belongie, James Hays, Pietro Perona, Deva Ramanan, Piotr Dollár, and C Lawrence Zitnick. Microsoft coco: Common objects in context. In *Computer Vision–ECCV 2014: 13th European Conference, Zurich, Switzerland, September 6–12, 2014, Proceedings, Part V 13*, pages 740–755, 2014.
- [52] Marius Cordts, Mohamed Omran, Sebastian Ramos, Timo Rehfeld, Markus Enzweiler, Rodrigo Benenson, Uwe Franke, Stefan Roth, and Bernt Schiele. The cityscapes dataset for semantic urban scene understanding. In *Proceedings of the IEEE/CVF conference on computer vision and pattern recognition*, pages 3213–3223, 2016.
- [53] Matthew Johnson-Roberson, Charles Barto, Rounak Mehta, Sharath Nittur Sridhar, Karl Rosaen, and Ram Vasudevan. Driving in the matrix: Can virtual worlds replace human-generated annotations for real world tasks? *arXiv preprint arXiv:1610.01983*, 2016.
- [54] Shuo Yang, Ping Luo, Chen-Change Loy, and Xiaoou Tang. Wider face: A face detection benchmark. In *Proceedings of the IEEE/CVF conference on computer vision and pattern recognition*, pages 5525–5533, 2016.
- [55] Christos Sakaridis, Dengxin Dai, and Luc Van Gool. Semantic foggy scene understanding with synthetic data. *International Journal of Computer Vision*, 126:973–992, 2018.
- [56] Naoto Inoue, Ryosuke Furuta, Toshihiko Yamasaki, and Kiyoharu Aizawa. Cross-domain weakly-supervised object detection through progressive domain adaptation. In *Proceedings of the IEEE/CVF conference on computer vision and pattern recognition*, pages 5001–5009, 2018.
- [57] Hajime Nada, Vishwanath A Sindagi, He Zhang, and Vishal M Patel. Pushing the limits of unconstrained face detection: a challenge dataset and baseline results. In *2018 IEEE 9th International Conference on Biometrics Theory, Applications and Systems (BTAS)*, pages 1–10, 2018.

- [58] Boyi Li, Wenqi Ren, Dengpan Fu, Dacheng Tao, Dan Feng, Wenjun Zeng, and Zhangyang Wang. Benchmarking single-image dehazing and beyond. *IEEE Transactions on Image Processing*, 28:492–505, 2018.
- [59] Shuai Shao, Zeming Li, Tianyuan Zhang, Chao Peng, Gang Yu, Xiangyu Zhang, Jing Li, and Jian Sun. Objects365: A large-scale, high-quality dataset for object detection. In *Proceedings of the IEEE/CVF international conference on computer vision*, pages 8430–8439, 2019.
- [60] Agrim Gupta, Piotr Dollar, and Ross Girshick. Lvis: A dataset for large vocabulary instance segmentation. In *Proceedings of the IEEE/CVF conference on computer vision and pattern recognition*, pages 5356–5364, 2019.
- [61] Chunyuan Li, Haotian Liu, Liunian Li, Pengchuan Zhang, Jyoti Aneja, Jianwei Yang, Ping Jin, Houdong Hu, Zicheng Liu, Yong Jae Lee, et al. Elevator: A benchmark and toolkit for evaluating language-augmented visual models. *Advances in Neural Information Processing Systems*, 35:9287–9301, 2022.
- [62] Yupeng Zhang, Shuqi Zheng, Ruize Han, Yuzhong Feng, Junhui Hou, Linqi Song, Wei Feng, and Liang Wan. Rethinking the one-shot object detection: Cross-domain object search. In *ACM Multimedia 2024*.
- [63] Shanshan Zhang, Rodrigo Benenson, and Bernt Schiele. Citypersons: A diverse dataset for pedestrian detection. In *Proceedings of the IEEE conference on computer vision and pattern recognition*, pages 3213–3221, 2017.
- [64] Piotr Dollár, Christian Wojek, Bernt Schiele, and Pietro Perona. Pedestrian detection: A benchmark. In *2009 IEEE conference on computer vision and pattern recognition*, pages 304–311, 2009.
- [65] Yanwei Pang, Jiale Cao, Yazhao Li, Jin Xie, Hanqing Sun, and Jinfeng Gong. Tju-dhd: A diverse high-resolution dataset for object detection. *IEEE Transactions on Image Processing*, 30:207–219, 2021.
- [66] Changfeng Yu, Shiming Chen, Yi Chang, Yibing Song, and Luxin Yan. Both diverse and realism matter: Physical attribute and style alignment for rainy image generation. In *Proceedings of the IEEE/CVF International Conference on Computer Vision*, pages 12387–12397, 2023.
- [67] Jing Zhang, Yang Cao, Shuai Fang, Yu Kang, and Chang Wen Chen. Fast haze removal for nighttime image using maximum reflectance prior. In *Proceedings of the IEEE conference on computer vision and pattern recognition*, pages 7418–7426, 2017.
- [68] Chao Dong, Chen Change Loy, Kaiming He, and Xiaoou Tang. Learning a deep convolutional network for image super-resolution. In *Computer Vision–ECCV 2014: 13th European Conference, Zurich, Switzerland, September 6–12, 2014, Proceedings, Part IV 13*, pages 184–199, 2014.
- [69] Christian Ledig, Lucas Theis, Ferenc Huszár, Jose Caballero, Andrew Cunningham, Alejandro Acosta, Andrew Aitken, Alykhan Tejani, Johannes Totz, Zehan Wang, et al. Photo-realistic single image super-resolution using a generative adversarial network. In *Proceedings of the IEEE conference on computer vision and pattern recognition*, pages 4681–4690, 2017.
- [70] Stamatis Lefkimmiatis. Universal denoising networks: A novel cnn-based network architecture for image denoising. *arXiv preprint arXiv:1711.07807*, 2017.
- [71] Jan Flusser, Sajad Farokhi, Cyril Höschl, Tomáš Suk, Barbara Zitova, and Matteo Pedone. Recognition of images degraded by gaussian blur. *IEEE transactions on Image Processing*, 25(2):790–806, 2015.
- [72] Jian Sun, Wenfei Cao, Zongben Xu, and Jean Ponce. Learning a convolutional neural network for non-uniform motion blur removal. In *Proceedings of the IEEE conference on computer vision and pattern recognition*, pages 769–777, 2015.
- [73] Mohsen Ebrahimi Moghaddam. A mathematical model to estimate out of focus blur. In *2007 5th International Symposium on Image and Signal Processing and Analysis*, pages 278–281, 2007.
- [74] Chengjian Feng, Yujie Zhong, Zequn Jie, Xiangxiang Chu, Haibing Ren, Xiaolin Wei, Weidi Xie, and Lin Ma. Promptdet: Towards open-vocabulary detection using uncured images. In *European conference on computer vision*, pages 701–717. Springer, 2022.
- [75] Liunian Li, Zi-Yi Dou, Nanyun Peng, and Kai-Wei Chang. Desco: Learning object recognition with rich language descriptions. *Advances in Neural Information Processing Systems*, 36:37511–37526, 2023.
- [76] Penghui Du, Yu Wang, Yifan Sun, Luting Wang, Yue Liao, Gang Zhang, Errui Ding, Yan Wang, Jingdong Wang, and Si Liu. Lami-detr: Open-vocabulary detection with language model instruction. In *European Conference on Computer Vision*, pages 312–328. Springer, 2024.

- [77] Sheng Jin, Xueying Jiang, Jiaying Huang, Lewei Lu, and Shijian Lu. Llms meet vlms: Boost open vocabulary object detection with fine-grained descriptors. *arXiv preprint arXiv:2402.04630*, 2024.
- [78] Jooyeon Kim, Eulrang Cho, Sehyung Kim, and Hyunwoo J Kim. Retrieval-augmented open-vocabulary object detection. In *Proceedings of the IEEE/CVF Conference on Computer Vision and Pattern Recognition*, pages 17427–17436, 2024.
- [79] Xun Huang and Serge Belongie. Arbitrary style transfer in real-time with adaptive instance normalization. In *Proceedings of the IEEE international conference on computer vision*, pages 1501–1510, 2017.
- [80] Kaiming He, Georgia Gkioxari, Piotr Dollár, and Ross Girshick. Mask r-cnn. In *Proceedings of the IEEE international conference on computer vision*, pages 2961–2969, 2017.
- [81] Fengchun Qiao, Long Zhao, and Xi Peng. Learning to learn single domain generalization. In *Proceedings of the IEEE/CVF conference on computer vision and pattern recognition*, pages 12556–12565, 2020.
- [82] Tianheng Cheng, Lin Song, Yixiao Ge, Wenyu Liu, Xinggang Wang, and Ying Shan. Yolo-world: Real-time open-vocabulary object detection. In *Proceedings of the IEEE/CVF Conference on Computer Vision and Pattern Recognition*, pages 16901–16911, 2024.
- [83] Tejas Gokhale, Rushil Anirudh, Jayaraman J Thiagarajan, Bhavya Kailkhura, Chitta Baral, and Yezhou Yang. Improving diversity with adversarially learned transformations for domain generalization. In *Proceedings of the IEEE/CVF Winter Conference on Applications of Computer Vision*, pages 434–443, 2023.
- [84] Sheng Cheng, Tejas Gokhale, and Yezhou Yang. Adversarial bayesian augmentation for single-source domain generalization. In *Proceedings of the IEEE/CVF International Conference on Computer Vision*, pages 11400–11410, 2023.

7 More Results

7.1 Comparison on LVIS

We further test our method on the LVIS validation set in Table 5. Our method (with ViT-L/14) also achieves the best overall AP among all methods. We can also see that when using the same backbone, the proposed method consistently outperforms CLIPSelf and F-VLM for all four settings. Overall, the performance gains of our method on LVIS are less pronounced compared to those on OD-LVIS. This is because of the lower domain diversity in LVIS, whereas our method demonstrates stronger competitiveness on more diverse OD-LVIS.

7.2 DG method comparison

In Table 6, we compare our method with two SOTA domain generalization (DG) methods based on CLIPSelf on OD-LVIS. It can be observed that our method achieves the best performance.

7.3 Visualization result analysis

As shown in Figures 4 and 5, we present the qualitative results of open-domain open-vocabulary object detection on OD-LVIS using both CLIPSelf [9] and our method. These visualizations highlight the models’ performance and their ability to detect novel objects. Notably, in certain complex scenarios, CLIPSelf struggles to effectively detect objects, whereas our method demonstrates superior adaptability, accurately identifying the majority of objects in more challenging environments.

Table 5: Comparison with SOTA on LVIS (%).

Method	Backbone	AP_f	AP_c	AP_r	AP
RegionCLIP [24]	RN50	34.0	27.4	17.1	28.2
RegionCLIP	RN50x4	36.9	32.1	22.0	32.3
OWL-ViT [25]	ViT-B/16	-	-	20.6	27.2
OWL-ViT	ViT-L/14	-	-	31.2	34.6
RKDWTF [26]	RN50 Base	26.4	19.4	12.2	20.9
RKDWTF	RN50 RKDPIS	25.5	20.9	17.3	22.1
RKDWTF	RN50 WTF	26.7	21.4	17.1	22.8
RKDWTF	RN50 WTF8x	29.1	25.0	21.1	25.9
MM-OVOD [28]	RN50_Avg	-	-	20.7	30.5
MM-OVOD	RN50_Agg	-	-	19.2	30.6
MM-OVOD	RN50_Avg_in-L	-	-	26.5	32.8
MM-OVOD	RN50_Agg_in-L	-	-	27.3	33.1
DK-DETR [29]	RN50	40.2	32.0	22.2	33.5
YOLO-World-L	YOLOv8-L	35.4	24.9	22.9	28.7
F-VLM	RN50x16	-	-	30.4	32.1
OV-DQUO [42]	ViT-B/16	23.8	27.7	29.4	26.5
OV-DQUO	ViT-L/14	28.5	36.0	39.5	33.7
ClipSelf [9]	ViT-B/16	29.1	21.8	25.3	25.2
ClipSelf	ViT-L/14	35.6	34.6	34.9	35.1
Ours (DAPmt + DP&G)	RN50x16	33.0	34.1	33.1	33.5
Ours (DAPmt + DP&G)	ViT-B/16	30.4	23.2	26.3	26.6
Ours (DAPmt + DP&G)	ViT-L/14	36.9	35.8	36.4	36.3

Table 6: Comparison with DG methods (%).

Method	Backbone	AP_f	AP_c	AP_r	AP
CLIPSelf (baseline)	ViT-B/16	17.1	12.0	12.2	14.0
+ ALT [83]	ViT-B/16	17.3	12.5	12.4	14.4
+ ABA [84]	ViT-B/16	18.2	13.3	13.1	15.2
Ours	ViT-B/16	19.0	14.3	14.0	16.1

Table 7: Cross-dataset main results on Objects365.

Method	Backbone	Training Data	AP_r	AP	AP^{50}
Detic	RN50*	LVIS-all	9.5	13.9	19.7
		LVIS-all + IN-L	12.4	15.6	22.2
MM-OVOD		LVIS-all	10.1	14.8	21.0
		LVIS-all + IN-L	13.1	16.6	23.1
F-ViT+CLIPSelf	ViT-B/16	LVIS-base	16.8	19.0	32.3
	ViT-L/14		21.7	23.7	39.2
ODOVD	RN50x16		18.2	19.9	34.1
	ViT-B/16		17.5	19.2	32.8
	ViT-L/14		22.3	24.0	39.7

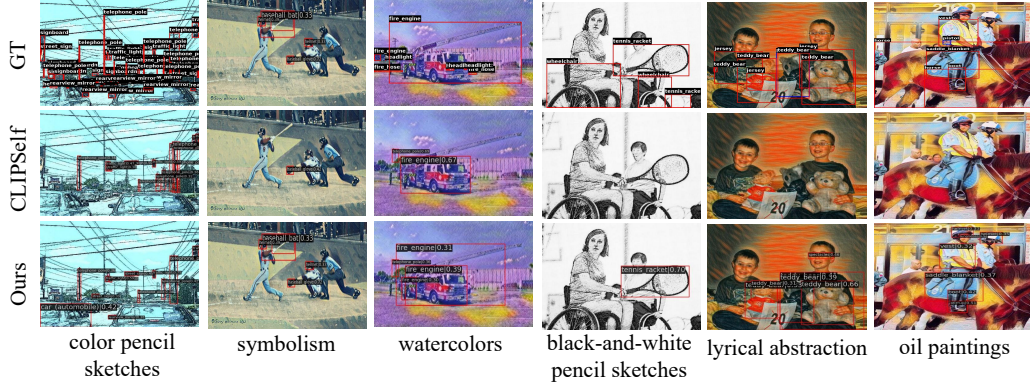


Figure 4: Visualization of open-domain open-vocabulary object detection results (under various image styles). We can see that, with the image style shift, many targets (such as the ‘car’ in the first column, and the ‘baseball bat’ in the second column) can not be detected by the CLIPSelf as shown in the second row. The proposed method can effectively detect these targets. More seriously, CLIPSelf can not identify any object under the more abstract styles, such as black-and-white pencil sketches, lyrical abstraction, and oil paintings as shown in the last three columns. The proposed method can identify many of the interested objects, which demonstrates our approach’s ability to detect the objects in complex and dynamic scenarios compared to previous methods. However, compared to the ground-truth results, our method also fails to detect many objects. This also indicates that the proposed ODOV is very difficult with much room for improvement.

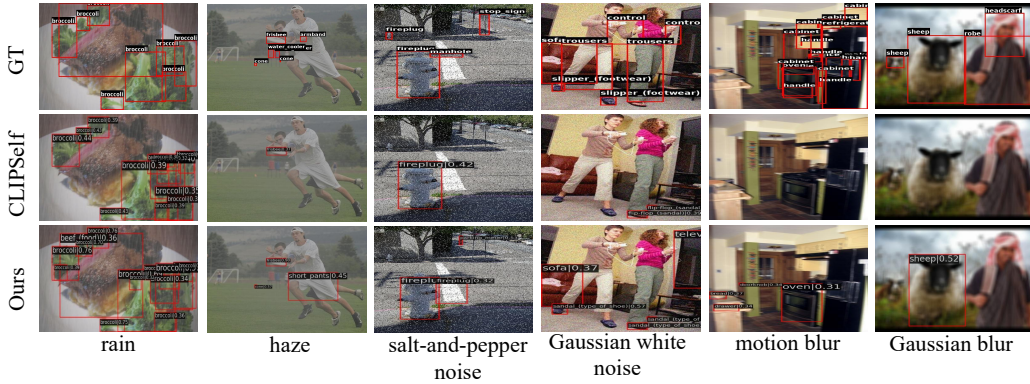


Figure 5: Visualization of open-domain open-vocabulary object detection results (under various imaging conditions). With the imaging condition shift, CLIPSelf performs well in some cases, such as the (light) rainy scene in the first column. It is partly influenced in the following cases, including the haze, salt-and-pepper noise, and Gaussian white noise, in which our method performs better to correctly detect more targets. As shown in the last two columns, the motion blur and Gaussian blur are severe, which makes the CLIPSelf difficult to detect the desired objects. Under these cases, our method can also identify some of them, which further demonstrates the effectiveness of our method.